Pacific Graphics 2012
C. Bregler, P. Sander, and M. Wimmer
(Guest Editors)

Volume 31 (2012), Number 7

Wetting Effects in Hair Simulation

W. Rungjiratananon[1], Y. Kanamori[2] and T. Nishita[1]

[1]The University of Tokyo, Japan
[2]University of Tsukuba, Japan

Abstract

There is considerable recent progress in hair simulations, driven by the high demands in computer animated movies. However, capturing the complex interactions between hair and water is still relatively in its infancy. Such interactions are best modeled as those between water and an anisotropic permeable medium as water can flow into and out of the hair volume biased in hair fiber direction. Modeling the interaction is further challenged when the hair is allowed to move. In this paper, we introduce a simulation model that reproduces interactions between water and hair as a dynamic anisotropic permeable material. We utilize an Eulerian approach for capturing the microscopic porosity of hair and handle the wetting effects using a Cartesian bounding grid. A Lagrangian approach is used to simulate every single hair strand including interactions with each other, yielding fine-detailed dynamic hair simulation. Our model and simulation generate many interesting effects of interactions between fine-detailed dynamic hair and water, i.e., water absorption and diffusion, cohesion of wet hair strands, water flow within the hair volume, water dripping from the wet hair strands and morphological shape transformations of wet hair.

Categories and Subject Descriptors (according to ACM CCS): I.3.7 [Computer Graphics]: Computer Graphics—Three-Dimensional Graphics and RealismAnimation

1. Introduction

Wetting of hair is an interesting phenomenon in our everyday life. When water contacts with hair, the water is absorbed and diffuses into the hair, making the hair wet. Then, the wet hair strands stick to surrounding strands and form several clumps due to cohesive forces caused by water bridges. The absorbed water also makes the hair strands heavier and temporally alters the protein structure (keratin) of a hair strand, causing its shape to change. For example, one's straight hair may turn into wavy hair or vice versa when wet. With enough water, the hair will be saturated and the excess water will flow down the hair strands to the tips. When the water at the tips grows large enough, it will turn into a water drop dripping out off the hair.

The permeability (the water absorption and diffusion) of hair originates in an inner part of each hair strand and a vast amount of microscopic void spaces among hair strands. Each hair strand is a permeable material which can absorb water up to 30%-45% of its mass [LÍ11] and the microscopic void spaces among hair strands form a porous structure similar to microscopic pores in porous materials such as sponges. These microscopic void spaces absorb and diffuse water due to a *capillary effect*. However, while pores in sponge-like objects do not move inside the solid material, void spaces in hair lie in complicated contact regions among hair strands and drastically change their position together with hair motion. Furthermore, hair is an anisotropic permeable medium; water diffuses more in the hair fiber direction than the orthogonal direction.

Recently, the coupling simulations between water and permeable media including water absorption and diffusion, such as sand [RSKN08, LD09] and sponge [LAD08], have been studied. However, these methods did not consider the special features of hair porosity mentioned above. These methods sampled permeable media in a macroscopic scale by particles [RSKN08] or *porous particles* [LAD08, LD09] with a diameter comparable to water particles to keep computational cost low. Note that a drop of water usually has a diameter around 2-5 mm [WMT05] which is fairly large compared to 15-110 μm of a hair strand [Rob02]. *Smoothed Particle Hydrodynamics* (SPH) [MCG03] is used for the water simulation in their works. We also follow their approach using SPH for water simulation and handle hair porosity at a

Figure 1: *A simulation result of 5,000 wavy hair strands with water showered onto them until completely wet. The water is absorbed and diffused, making the hair wet and saturated, then the excess water flows along the hair strands until dripping out at the tips. The wet hair strands stick to surrounding strands forming several clumps, while the detail of some wet stray hair forming a clump can be seen as well.*

macroscopic scale. We model the porosity of hair volume using a Cartesian bounding grid, because it is difficult to sample hair volume that is not continuum by particles. Then, our model introduces a method to capture the porosity of hair volume and a method to handle wetting effects of hair on the grid.

While the wetting effects of hair are handled by an Eulerian approach, we use a Lagrangian approach to simulate every single hair strand as an individual entity, yielding the best plausible results of fine-detailed hair dynamics. There are several models for strand dynamics such as mass-spring model [SLF08], super-helices [BAC*06] and shape matching based model [RKN10]. In this paper, we use the shape matching based model called *Chain Shape Matching* (CSM). The CSM can efficiently handle individual hair strands as well as an easy shape controllability of hair strands which advantages morphological shape transformation of wet hair in our model. An interesting interactions between fine-detailed hair and water can be handled by our method as shown in Figure 1. Hair is wet by the water absorption and diffusion. Wet hair strands stick to surrounding strands as expected and a detail of stray hair between clumps of wet hair can be seen as well.

Our contribution is a simulation model that reproduces full interactions between hair and water. We introduce a method that captures the wetting effects of fine-detailed dynamic hair simulation using a Cartesian bounding grid. Hair can be handled as a dynamics anisotropic permeable material with our model. The complex porous structure of hair can be captured even under the motion. Our model recreates many interesting wetting effects of hair, i.e., water absorption and diffusion, cohesion of wet hair strands, water flow within the hair volume, water dripping from the wet hair strands and morphological shape transformations of wet hair.

2. Related Work

Most of previous work regarding wet hair did not target simulations but focused on rendering [GMT07] and modeling [Bru00, SBCN10]. Only a few research studies have been introduced for the dynamics of strand-like objects with wetting effects. Procedural techniques were proposed for modeling clumping of wet fur [Bru00, SBCN10]. Ward et al. [WL04, WGL07] introduced a method for simulating wet hair whose wetness is supplied by user interactions. Their method is a clump-based model which sacrifices detail for speed. None of these methods is a full simulation between hair and water. To the best of our knowledge, the method of Ward et al. [WGL07] is the latest approach in wet hair simulation model.

Strand dynamics: Rosenblum et al. [RCT91] and Anjyo et al. [AUK92] are among the first groups that introduced methods for handling the dynamics of individual hair strand using mass-spring system and projective dynamics, respectively. There are also several works representing a hair strand as a serial chain of rigid bodies [CCK05, Had06] or elastic rod [Pai02, BAC*06, ST07]. Mass-spring system is extended by Selle et al. [SLF08] to enable torsion and solve numerical stability problem. McAdams et al. [MSW*09] introduced a hybrid Eulerian/Lagrangian method to efficiently capture the interactions among straight hair strands. To speed up simulations, several techniques reduce degrees-of-freedom of hair using clump based models [DTKT93, BKCN03, Osh07] or a continuum models [BNC03, VMT06]. Alternatively, Rungjiratananon et al. [RKN10] introduced a Chain Shape Matching (CSM) model to simulate each single individual hair strand. The CSM can directly modify positions of hair particles; therefore transforming wet hair shape during the simulation is straightforward. Our Eulerian method for wetting effects can be applied to any hair simulation models. However, considering morphological shape transformation of wet hair, the CSM is our appropriate choice.

Porous media and water simulation: The wetting effects in porous media and water simulation has been studied recently. Rungjiratananon et al. [RSKN08] introduced a particle-based model for sand-water interactions. Lenaerts et al. [LAD08] integrated porous flow into SPH framework for permeable media (rigid and elastic bodies) and water simulation. Later, Lenaerts et al. [LD09] applied their framework to porous flow in granular material such as sand. Their methods sample solid permeable media in a macroscopic scale by particles and handle wetting effects as an interactions between particles. However, these models do not consider the dynamic anisotropic porous medium such as hair. Huber et al. [HPS11] introduced a simulation model for wet cloth including water absorption, diffusion and stickiness. However, their model is limited to wetting effects on a flat surface.

3. Overview

To model wetting effects in coupling simulations of hair and water, our method introduces a Cartesian grid to implicitly represent the dynamic capillary system among hair strands (Section 4). Each voxel in this grid defines the unit for water absorption and diffusion. Water travels in the hair volume both in microscopic (hair strands) and macroscopic scales (voxels). In the microscopic scale, each hair segment of each hair strand holds some water inside and around the segment. The water inside the segment diffuses to adjacent segments in a hair strand, and the water around the segment flows along the hair strand. In the macroscopic scale, each voxel containing hair absorbs water and the water diffuses among voxels. The water in each voxel is then distributed to each segment within the voxel. The water propagation processes are summarized in the following four stages:

Voxel absorption: When water contacts with voxels, the water is absorbed to the voxel (Section 5.1).

Macroscopic propagation (Inter-voxel diffusion): The water propagates to the neighboring voxels according to the difference of capillaries of the voxels (Section 5.2). The change of water in each voxel is then distributed to segments in the voxel.

Microscopic propagation: Water inside each segment diffuses to its connected segments and the excessive water around the segment flows along the hair strand, which is followed by intra-voxel diffusion that uniformizes segments' water amount within the voxel (Section 5.3).

Water dripping: Water drips out as a droplet from a voxel if the water mass exceeds its capacity in certain duration. (Section 5.4).

After these processes, the stored water in each segment causes cohesion forces (Section 6) and morphological shape transformation (Section 7) as well as increase of the weight of hair strands. Algorithm 1 shows the pseudocode of our algorithm.

Algorithm 1 Pseudocode of our algorithm.

Given V: a set of non-empty voxels.
Given M: hair surface meshes (Section 5.4).
Given w_i: current water mass in segment i
Given w_v: current water mass in voxel v
Given W_v: a set of water capacities in voxel v
loop
    SIMULATECSMANDSPH()
    $V, w_v, W_v \leftarrow$ CONSTRUCTGRID() // Section 4
    for all voxel $v \in V$ **do**
        VOXELABSORPTION(w_v, W_v) // Section 5.1
        INTERVOXELDIFFUSION(w_v, W_v) // Section 5.2
        for all segment i in voxel v **do**
            $w_i \leftarrow w_i +$ INTERPOLATECHANGE()
            INSIDEHAIRSTRANDDIFFUSION(w_i)
        end for
    end for
    for all segment i **do**
        FREEWATERFLOW(w_i) // Section 5.3
    end for
    for all voxel $v \in V$ **do**
        INTRAVOXELDIFFUSION() // Section 5.3
    end for
    $M \leftarrow$ CONSTRUCTHAIRSURFACE()
    DRIPWATER(M) // Section 5.4
    for all segment i **do**
        COMPUTECOHESIONFORCES() // Section 6
        SHAPETRANSFORM() // Section 7
    end for
end loop

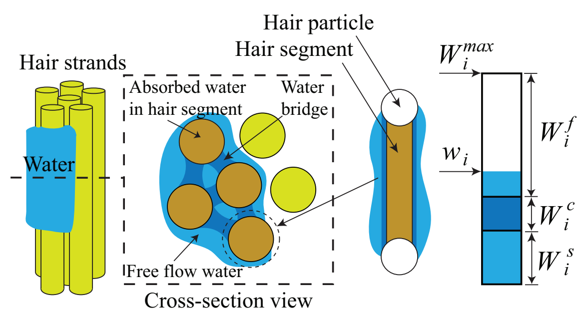

Figure 2: *A brief microscopic illustration of wet hair and our simulation model of a hair segment. Water permeated into hair is represented as a water mass of a hair segment. The total possible amount of water mass is a summation of absorbed water, water bridge and free-flow water capacities.*

4. Grid Construction

As introduced in Section 1, when water contacts with hair, the water absorption and diffusion happens due to the permeability of hair strands and capillaries. However, the capillaries of hair is difficult to figure out due to the complexity of hair structure. We can do nearest neighbors search for each hair segment and examine contact regions among neighboring hair segments to accurately determine the capillaries, but it is not an efficient way. Therefore, we introduce a grid of uniform voxels to approximate the capillaries of hair.

Hair volume is divided into voxels. Each voxel contains portions of hair segments and acts as a *porous voxel* that absorbs and diffuses water. In a porous voxel v, the maximum water capacity W_v^{max} that a porous voxel v can hold is considered as a summation of three capacities of water as follows (see Figure 2).

- **Water capacity in hair segments** W_v^s: The water capacity can be held inside of the hair segments.
- **Water capacity in capillaries** W_v^c: The water capacity held by capillaries (the extremely small gaps) between hair segments. We call the water in the capillaries *water bridges*.
- **Water capacity of free flow** W_v^f: The capacity of water around the hair segments that is not absorbed into hair segments or held as water bridges, but covers the hair segments due to a cohesion. This capacity is a user-defined value controlling the amount of water considered as an Eulerian free-flow water.

Regarding notations, we use capitalized W for water capacity and small w for current water amount. Superscripts s, c and f denote water in *segments*, *capillaries* and *free flow*, respectively. Additionally, subscripts v and i indicate water in a *voxel* and a *segment*, respectively.

The maximum capacity of the voxel is then: $W_v^{max} = W_v^s + W_v^c + W_v^f$. The W_v^s and W_v^f can be directly computed from a function of the total mass of hair in the voxel, while the capacity of capillaries W_v^c is approximated.

To determine the total hair mass in the voxel, we rasterize each hair segment in the grid using *3D Digital Differential Analyzer* (3DDDA). 3DDDA yields a set of voxels that segment i passes through together with its length in each voxel. Let l_{iv} be a length of segment i in a voxel v (Figure 3), then the total length of hair segments L_v and total mass of hair m_v^{hair} in the voxel can be computed as follows.

$$L_v = \sum_{i \in \mathcal{R}(v)} l_{iv}, \tag{1}$$

$$m_v^{hair} = \rho_{hair} \pi r^2 L_v, \tag{2}$$

where $\mathcal{R}(v)$ is a set of segments in the voxel v, ρ_{hair} is the density of hair segment and r is a radius of cylindrical hair segment. Then, we can compute water capacity in portions of hair segments W_v^s and free-flow water capacity W_v^f as follows.

$$W_v^s = K_{hair} m_v^{hair}, \tag{3}$$

$$W_v^f = k_{free} m_v^{hair}, \tag{4}$$

where K_{hair} is a permeability of a hair segment (usually $0.3 \leq K_{hair} \leq 0.45$, as described in Section 1) and k_{free} is a constant controlling the free-flow water capacity.

To approximate W_v^c, we assume that the contact regions of hair strands are proportional to the total mass of hair inside the voxel.

$$W_v^c = \begin{cases} 0, & \text{if } |\mathcal{R}(v)| = 1 \\ k_{capillaries} m_v^{hair}, & \text{otherwise} \end{cases} \tag{5}$$

where $k_{capillaries}$ is a constant and $|\mathcal{R}(v)|$ is the number of segments in the voxel v. Our simple assumption is based on the fact that wet hair segments tend to stick to each other such that the water bridges totally lie in the clump of hair strands. The higher the number of hair strands in the clump is, the larger the water bridges are. However, it might result in a large error according to complicated configuration of dry hair strands. The more accurate method for approximating topology of contact region inside the voxel is one of our future work.

In our model, a hair segment i stores water mass w_i. The current amount of water mass w_v in a voxel can be computed from a summation of water mass of the portions of segments in the voxel. We consider that the water mass of a segment is uniformly distributed in the segment (Figure 3), therefore a water mass of a portion of the segment is linear proportional to its length.

$$w_v = \sum_{i \in \mathcal{R}(v)} w_i \frac{l_{iv}}{l_i}, \tag{6}$$

where l_i is the total length of segment.

Later in this paper, the current amount of water mass in each capacity is used to handle the wetting effects. We define the current amount of each kind of water mass as follows.

$$w_v^s = \min\{w_v, W_v^s\}, \tag{7}$$

$$w_v^c = \min\{\max\{0, w_v - W_v^s\}, W_v^c\}, \tag{8}$$

$$w_v^f = \max\{0, w_v - W_v^s - W_v^c\}. \tag{9}$$

Equations 7, 8 and 9 represent the current water mass of each kind in the voxel. We use the same equations for the current water amount of a segment as well, i.e., w_i^s, w_i^c and w_i^f.

To handle an anisotropic water diffusion in hair, a representative tangent vector of hair in each voxel has to be known. We use an averaged tangent vector $\mathbf{d}_v$ of each segment in the voxel as the representative tangent vector.

$$\mathbf{d}_v = \frac{1}{L_v} \sum_{i \in \mathcal{R}(v)} \mathbf{u}_i \frac{l_{iv}}{l_i}, \tag{10}$$

where $\mathbf{u}_i$ is the tangent vector of segment i.

5. Water Propagation

Water flows into and drips out of the hair volume influenced by voxel absorption, macroscopic and microscopic water propagation. In this section, we describe the detail of each stage.

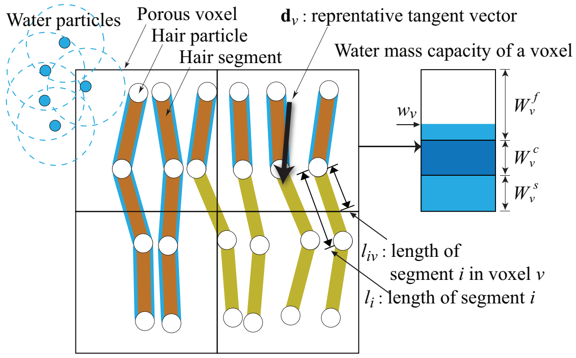

Figure 3: *An Eulerian grid of uniform voxels for capturing hair porosity. Each voxel contains portions of hair segments.*

5.1. Voxel Absorption

When a water particle p contacts with a porous voxel v, we consider the following conditions to check whether the water particle gets absorbed or not.

- The porous voxel has a capacity left, i.e., $w_v < W_v^{max}$.
- The water particle's velocity $\mathbf{v}_p$ is toward the porous voxel, i.e., $\mathbf{v}_p \cdot \mathbf{n}_{pv} > 0$, where $\mathbf{n}_{pv}$ is the vector from the water particle to the center of the porous voxel.

When the water particle is absorbed into the porous voxel, the water mass of the porous voxel is increased by the water particle's mass $w_v \leftarrow w_v + w_{SPH}$, where w_{SPH} is the water mass of the water particle (Figure 3).

5.2. Macroscopic Propagation

The difference of water in capillaries between the porous voxels is the main cause of the inter-voxel diffusion. We employ the Fick's second law for the change of the water in capillaries over time.

$$\frac{\partial w_v^c}{\partial t} = \nabla \cdot (D_v \nabla w_v^c), \tag{11}$$

where D_v is the diffusivity of porous voxel. The diffusivity of an isotropic porous voxel can be some constant. However, hair is an anisotropic permeable medium where the water diffuses more in the hair tangent direction. Given $D_{\|}$ and $D_{\perp}$ are diffusivity constants in the hair tangent and orthogonal directions, respectively, we modify the diffusivity for an anisotropic porous voxel as follows.

$$D_v = D_{\|}\lambda + D_{\perp}(1-\lambda), \tag{12}$$
$$\lambda = |\mathbf{d}_v \cdot \mathbf{u}|, \tag{13}$$

where $\mathbf{u}$ is the unit vector from the voxel v to a neighboring voxel. The evolution of diffused water mass, Δw_v, is then computed on the grid as follows.

$$\frac{\Delta w_v}{\Delta t} = \sum_{u \in \mathcal{G}(v)} D_v (S_u - S_v) \frac{(w_u^c - w_v^c)}{\Delta d}, \tag{14}$$

where $\mathcal{G}(v)$ is a set of six connected neighboring voxels of voxel v, Δt is a time step, Δd is a size of voxel, and S_v is a saturation of the voxel v. The saturation is a mass fraction of water in the capillaries of the porous voxel: $S_v = \frac{w_v^c}{W_v^c}$.

After the absorption and diffusion processes, we update the change of water mass in each porous voxel Δw_v to segments in the voxel. The increase is distributed to each segment according to the fraction of its portion length in the voxel (Eq. 15). The longer the portion is, the more change is distributed to that segment.

$$\Delta w_i^{increase} = \sum_{v \in \mathcal{G}(i)} \Delta w_v \frac{l_{iv}}{L_v}, \tag{15}$$

where $\mathcal{G}(i)$ is a set of voxels that segment i passes through. However, there's possibly a problem in case that the change of water mass is decreasing and some segments in the voxel has no water mass. The water mass of those segments will be updated to a negative value, which is impossible. Therefore, we use a fraction of water mass that the segment contributes to the voxel w_{iv} for the change (Eq. 16), instead of the fraction of length.

$$\Delta w_i^{decrease} = \sum_{v \in \mathcal{G}(i)} \Delta w_v \frac{w_{iv}}{w_v}. \tag{16}$$

5.3. Microscopic Propagation

In microscopic level, we consider the diffusion of water inside a segment w_i^s and the flow of free-flow water w_i^f. For each segment, there are also three kinds of water mass capacity. W_i^s and W_i^f are directly computed from the mass of the hair segment, while W_i^c is derived from the approximated W_v^c in the voxels (Eq. 5) that the segment resides in.

$$W_i^c = \sum_{v \in \mathcal{G}(i)} W_v^c \frac{l_{iv}}{l_i}. \tag{17}$$

As a result, the current amount of water inside the segment w_i^s and free-flow water mass of the segment w_i^f can be calculated similarly to Eq. 7 and 9, respectively.

The current water mass inside the segment diffuses to the adjacent segments in its strand. We use a simple diffusion process as follows.

$$\frac{\Delta w_i}{\Delta t} = D_s (w_{i+1}^s + w_{i-1}^s - 2w_i^s), \tag{18}$$

where Δw_i is the variation of w_i and D_s is a diffusivity between hair segments.

The water that flows within the hair volume is the free-flow water of the segment, w_i^f. We move this free-flow water along a hair strand from segment to segment controlled by a flow rate k_{flow} and the direction of the segment. We determine the direction of the flow by checking the dot product of the unit tangent vector of hair segment $\mathbf{t}_i$ and the unit gravity direction $\hat{\mathbf{g}}$, i.e., $k_{dir} = \mathbf{t}_i \cdot \hat{\mathbf{g}}$.

1. There will be no flow, if $|k_{dir}|$ is less than a threshold ε.
2. If $k_{dir} \geq \varepsilon$, the water will flow to the next segment, $w_{i+1} \leftarrow w_{i+1} + \Delta t k_{flow} |k_{dir}| w_i^f$.
3. If $k_{dir} \leq -\varepsilon$, the water will flow to the previous segment, $w_{i-1} \leftarrow w_{i-1} + \Delta t k_{flow} |k_{dir}| w_i^f$.

Each segment transfers an amount of free-flow water from voxels to voxels. The update of the water mass w_v in each voxel can be computed using Eq. 6. The free-flow water inside the voxel diffuses among the segments as well, e.g., there might be free-flow water inside the voxel that has dry segments. We update w_i of each segment as follows.

$$\Delta w_i = \Delta t k_f \left(w_v^f \frac{l_{iv}}{L_v} - w_i^f \frac{l_{iv}}{l_i}\right), \tag{19}$$

where k_f is a constant. The first term on the right hand side in Eq. 19 is the probable free-flow water mass of the segment when all segments in the voxel are equally wet. The second term is the current free-flow water mass that the segment contributes to the voxel. The equation can be interpreted that the free-flow water mass of each segment gradually becomes equal to each other.

5.4. Water Dripping

Water droplets drips out when the water mass in a voxel exceeds W_v^{max}. Water droplets should be created around hair strands, but voxels are too coarse to specify where hair strands exist. For this, we create a surface mesh from the hair volume using distance transform of hair segments and the marching cubes algorithm [LC87]. We refer to this mesh as the *hair surface mesh*. If $w_v > W_v^{max}$ in voxel v and a hair surface mesh exists within the voxel, we generate a water particle and decrease the water mass of the voxel by the water particle's mass, $w_v \leftarrow w_v - w_{SPH}$. The decrease of the water mass is interpolated back to the segments in the voxel using Eq. 16. The position of the generated water particle is an averaged barycenter of the surface meshes (Figure 4). If there is a water particle within a water particle's radius of the generated position, we add radius and mass to the water particle instead of creating a new one.

To guarantee that absorbed water does not turn into water particles repeatedly or vice versa at the interface between porous voxels and water particles, we add a time delay γ. Dripping occurs if the voxel has the water mass exceeded W_v^{max} for γ time steps. We also add a small velocity to the generated water particle in the direction of an averaged normal vector of the surface meshes to avoid the absorption of generated water particles.

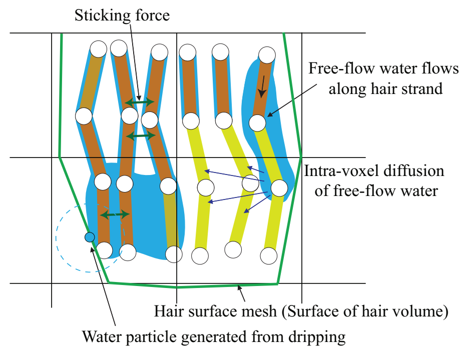

Figure 4: *Handling free flow water and cohesion of wet hair.*

6. Cohesion of Wet Hair

Cohesion of wet hair is influenced by the water bridges and the free-flow water. We add a sticking force between a pair of colliding segments according to those water masses of the segments (Figure 4). For collision detection we consider a hair segment as a *capsule* (a cylinder with two spheres at its endpoints). Let r be the cylindrical (and spherical) radius. The result of the collision detection gives the closest points $\mathbf{x}_i$ and $\mathbf{x}_j$ on the segments i and j, respectively. The pair of segments is a colliding pair when the length of the vector $\mathbf{x}_{ij} = \mathbf{x}_i - \mathbf{x}_j$ is less than d_{ij}, where d_{ij} is a distance taking into account the cylindrical radius r and the water amount.

$$d_{ij} = 2r + \sigma(w_i + w_j), \tag{20}$$

where σ is a ratio of increasing water radius. The sticking force between segments i and j is computed when $d_{ij} \geq |\mathbf{x}_{ij}| > 2r$:

$$\mathbf{F}_{ij}^{stick} = \frac{1}{2} k_{stick}(w_i + w_j)(d_{ij} - |\mathbf{x}_{ij}|)\frac{\mathbf{x}_{ij}}{|\mathbf{x}_{ij}|}, \tag{21}$$

where k_{stick} is a coefficient of the sticking force. If $|\mathbf{x}_{ij}| < 2r$, the penalty force is computed:

$$\mathbf{F}_{ij}^{penalty} = k_p(2r - |\mathbf{x}_{ij}|)\frac{\mathbf{x}_{ij}}{|\mathbf{x}_{ij}|}, \tag{22}$$

where k_p is a coefficient of the penalty force.

7. Morphological Shape Transformation

The absorbed water inside a hair strand can temporally alter the shape of wet hair due to chemical reactions. In the CSM model, a user assigns a predefined shape of a hair strand by giving positions of hair particles or tangent vectors of hair segments (see Figure 5). When the hair particles are moved by external forces, CSM tries to maintain the predefined shape. Accordingly, we assign two predefined shapes for a dry hair strand and a wet hair strand. When the hair segment i is wet, we first calculate a tangent vector that segment i should transforms into, called *goal tangent* $\mathbf{t}_i^{goal}$. The goal

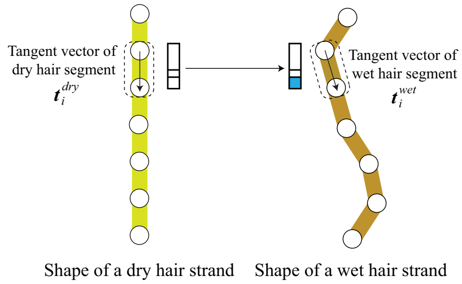

Figure 5: *Morphological shape transformation of wet hair. Predefined shapes of dry hair and wet hair are assigned by the user.*

Figure 6: *Comparison of our simulation results and real world experiments.*

Figure 7: *Results of morphological shape transformations in our model. The wet parts of straight hair (left) and curly hair (right) turn into wavy and straight hair, respectively.*

(a) With water repellent (b) Without water repellent

Figure 8: *Simulation results of hair with and without water repellent.*

tangent is interpolated between the tangent of dry segment $\mathbf{t}_i^{dry}$ and wet segment $\mathbf{t}_i^{wet}$ using the absorbed water mass inside the segment w_i^s. The current tangent vector $\mathbf{t}_i$ is then updated towards $\mathbf{t}_i^{goal}$ as follows.

$$\mathbf{t}_i^{goal} = (1 - \frac{w_i^s}{W_i^s})\mathbf{t}_i^{dry} + \frac{w_i^s}{W_i^s}\mathbf{t}_i^{wet}, \quad (23)$$

$$\mathbf{t}_i \leftarrow k_t \Delta t(\mathbf{t}_i^{goal} - \mathbf{t}_i), \quad (24)$$

where k_t is a constant controlling speed of the chemical reactions of hair strand.

8. Results

Our implementation was written in C++ with OpenGL. All experiments were conducted on a PC with an Intel Core i7 3.20GHz, 6GB RAM and an NVIDIA GeForce GTX 480 GPU. We use the *Dynamic Packing Grid* (DPG) data structure [BCR09] for a memory-efficient grid structure in our simulation. Our final results are rendered using an off-line rendering software, POVRay 3.7. Each hair segment is rendered as a semi-transparent cylinder. The color of a hair segment gets darker according to the amount of absorbed water mass. When the amount of free-flow water around a hair segment is large enough, the free-flow water can be seen as a thin water film covering the segment. In our rendering, we add some virtual water particles (not used for simulation, only for rendering) along the hair segment with the size according to the free-flow water amount. Then, we employ the method proposed in [YT10] for constructing the surfaces of water particles in SPH domain and virtual particles around hair segments.

Our simulation result compared with the real world is shown in Figure 6. The real hair and our results are shown in the left and right columns, respectively. The top row shows dry hair and the bottom row shows wet hair. There are 5,500 hair strands in the simulation result compared to over 100,000 strands of the real hair and the shape of hair strands are not exactly the same. Therefore, the overall appearance may look different. However, our method can reproduce the cohesion of wet hair and the presence of droplet at the tips as seen in the real hair.

Figure 7 shows results of morphological shape transformations according to the absorbed water. Straight hair temporally turns into wavy hair in Figure 7(left), while the wet curly hair in Figure 7(right) becomes more straight. In the curly hair, hair strands become straight due to the weight of the absorbed water and the morphological shape transformations, but largely induced by the shape transformations. Figure 9 shows results of 5,500 straight hair strands rising from a pool. Hair is completely wet under the water. The water amount in hair volume is maximum. Therefore, a great amount of excess water (free-flow water) flows along hair strands until pouring out of the hair volume when hair is rising into the air. Figure 10 shows animation sequences of 6,500 wavy hair strands interacting with water from a shower. The water is absorbed and diffuses into the hair. The wet hair strands form several clumps. The excess water gradually drips at the tips. The breakdown computational time in each process is shown in Table 1. The grid resolution used in Figures 7, 9 and 10 is $55 \times 55 \times 55$.

9. Discussions and Limitations

There are much more underlying physics of water and hair interactions in the real world, e.g., water repellent, surface tension between fluid and hair. In the real hair, there is sometimes a water repellent, i.e., water is repelled by the oil component or static electric in the hair. We demonstrate a simple way to handle this in Figure 8. We give each hair segment an α value that indicates the strength of oil component (or static electric) of the segment. The voxel absorption occurs only when the summation of α values in the voxel is less than a threshold. Unless, the α values of segments in the voxel keep decreasing when the voxel contacts with water.

Regarding the choice of voxel size, we use the size equal to or larger than a diameter of water particle, since a water particle can be totally absorbed into a voxel. Although the overall water mass in the hair volume remains the same with a larger voxel size, the water absorption and diffusion processes affect more hair segments in a time step. The computational cost of hair voxelization glows linearly together with the number of voxels.

10. Conclusion and Future Work

We have introduced a model for handling the wetting effects in coupling simulations of hair and water. Hair is modeled as an anisotropic dynamics permeable media. We have proposed a method utilizing Eulerian approach for capturing hair porosity and handling wetting effects on the fine detailed hair simulation using Lagrangian method. Our method have enabled many interesting effects of wetting hair. To the best of our knowledge, our system is the first to fully simulate the interactions between hair and water both in macroscopic and microscopic levels.

For future work, we would like to improve an overall performance by GPU implementation. In this paper, the approximation of capillaries among hair strands is based on a simple assumption. A more accurate and efficient method is required to capture the exact topology of capillaries among hair.

Acknowledgment

This work was supported in part by Grant-in-Aid for JSPS Fellows (22·4748).

References

[APKG07] ADAMS B., PAULY M., KEISER R., GUIBAS L. J.: Adaptively sampled particle fluids. In *SIGGRAPH '07: ACM SIGGRAPH 2007 papers* (2007), p. 48.

[AUK92] ANJYO K., USAMI Y., KURIHARA T.: A simple method for extracting the natural beauty of hair. In *SIGGRAPH '92: ACM SIGGRAPH 1992 Papers* (1992), ACM, pp. 111–120.

[BAC*06] BERTAILS F., AUDOLY B., CANI M.-P., QUERLEUX B., LEROY F., LÉVÊQUE J.-L.: Super-helices for predicting the dynamics of natural hair. *ACM Transactions on Graphics (SIGGRAPH) 25*, 3 (2006), 1180–1187.

[BCR09] BAJAJ C., CHOWDHURY R. A., RASHEED M.: A dynamic data structure for flexible molecular maintenance and informatics. In *2009 SIAM/ACM Joint Conference on Geometric and Physical Modeling* (2009), pp. 259–270.

[BKCN03] BERTAILS F., KIM T.-Y., CANI M.-P., NEUMANN U.: Adaptive wisp tree: a multiresolution control structure for simulating dynamic clustering in hair motion. In *Proceedings of the 2003 ACM SIGGRAPH/Eurographics symposium on Computer animation* (2003), pp. 207–213.

[BNC03] BANDO Y., NISHITA T., CHEN B.-Y.: Animating hair with loosely connected particles. *Computer Graphics Forum (Proceedings of EUROGRAPHICS 2003) 22*, 3 (2003), 411–418.

[Bru00] BRUDERLIN A.: A method to generate wet and broken-up animal fur. *Journal of Visualization and Computer Animation 11*, 5 (2000), 249–259.

[BWR*08] BERGOU M., WARDETZKY M., ROBINSON S., AUDOLY B., GRINSPUN E.: Discrete elastic rods. *ACM Transactions on Graphics (SIGGRAPH) 27*, 3 (aug 2008), 63:1–63:12.

[CCK05] CHOE B., CHOI M. G., KO H.-S.: Simulating complex hair with robust collision handling. In *SCA '05: Proceedings of the 2005 ACM SIGGRAPH/Eurographics symposium on Computer animation* (2005), ACM, pp. 153–160.

[DBB09] DIZIOL R., BENDER J., BAYER D.: Volume conserving simulation of deformable bodies. In *Eurographics 2009 Short Papers* (March 2009).

[DTKT93] DALDEGAN A., THALMANN N. M., KURIHARA T., THALMANN D.: An integrated system for modeling, animating and rendering hair. *Computer Graphics Forum 12*, 3 (1993), 211–221.

[GMT07] GUPTA R., MAGNENAT-THALMANN N.: Interactive rendering of optical effects in wet hair. In *Proceedings of the 2007 ACM symposium on Virtual reality software and technology* (2007), pp. 133–140.

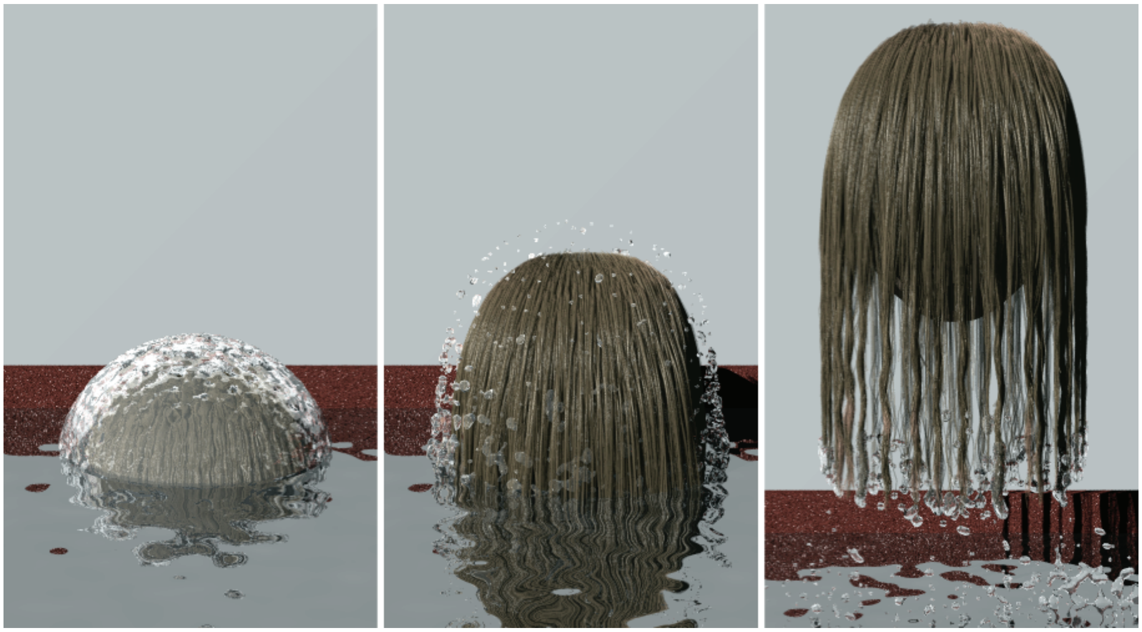

Figure 9: *Animation sequences of 5,500 wavy hair strands (105,000 segments) rising from a pool.*

Figure 10: *Animation sequences of 6,500 straight hair strands (134,000 segments) interacting with water from a shower.*

[Had06] HADAP S.: Oriented strands: dynamics of stiff multi-body system. In *Proceedings of the 2006 ACM SIGGRAPH/Eurographics Symposium on Computer Animation* (2006), pp. 91–100.

[Hil06] HILFER R.: Macroscopic capillarity and hysteresis for flow in porous media. *Phys. Rev. E 73* (Jan 2006), 016307.

[HPS11] HUBER M., PABST S., STRASSER W.: Wet cloth simulation. In *Computer Graphics International Workshop* (2011).

[LÍ1] LÓREAL.: Unexpected properties of hair, http://www.hair-science.com.

[LAD08] LENAERTS T., ADAMS B., DUTRÉ P.: Porous flow in particle-based fluid simulations. In *SIGGRAPH '08: ACM SIG-*

Table 1: *The computational time in seconds taken in each process.*

No. of hair segments / Max no. of water particles	CSM	SPH	Voxelization	Water absorption and diffusion	Water flow	Collisions and cohesions	Total time
15,000 segments / 2,500 particles (Figure 7)	0.034	0.098	0.331	0.003	0.005	0.470	0.941
105,000 segments / 8,200 particles (Figure 9)	0.185	0.212	3.182	0.009	0.034	3.797	7.419
134,000 segments / 9,500 particles (Figure 10)	0.239	0.284	3.872	0.015	0.037	4.126	8.573

GRAPH 2008 papers (2008), ACM, pp. 1–8.

[LC87] LORENSEN W. E., CLINE H. E.: Marching cubes: A high resolution 3d surface construction algorithm. *COMPUTER GRAPHICS 21*, 4 (1987), 163–169.

[LD09] LENAERTS T., DUTRÉ P.: Mixing fluids and granular materials. *Computer Graphics Forum (Proceedings of Eurographics 2009) 28*, 2 (2009), 213–218.

[MCG03] MÜLLER M., CHARYPAR D., GROSS M.: Particle-based fluid simulation for interactive applications. In *SCA '03: Proceedings of the 2003 ACM SIGGRAPH/Eurographics symposium on Computer animation* (2003), pp. 154–159.

[MHHR07] MÜLLER M., HEIDELBERGER B., HENNIX M., RATCLIFF J.: Position based dynamics. *Journal of Visual Communication and Image Representation 18*, 2 (2007), 109–118.

[MSKG05] MÜLLER M., SOLENTHALER B., KEISER R., GROSS M.: Particle-based fluid-fluid interaction. In *SCA '05: Proceedings of the 2005 ACM SIGGRAPH/Eurographics symposium on Computer animation* (2005), pp. 237–244.

[MSW*09] MCADAMS A., SELLE A., WARD K., SIFAKIS E., TERAN J.: Detail preserving continuum simulation of straight hair. *ACM Trans. Graph. 28* (2009), 62:1–62:6.

[NB] NITAO J. J., BEAR J.: Potentials and Their Role in Transport in Porous Media. *Water Resources Research 32*, 2, 225–250.

[Osh07] OSHITA M.: Real-time hair simulation on GPU with a dynamic wisp model. In *Comput. Animat. Virtual Worlds* (2007), vol. 18, John Wiley & Sons, Ltd., pp. 583–593.

[Pai02] PAI D. K.: Strands: Interactive simulation of thin solids using cosserat models. *Computer Graphics Forum 21*, 3 (2002), 347–352.

[RCT91] ROSENBLUM R. E., CARLSON W. E., TRIPP E.: Simulating the structure and dynamics of human hair: Modelling, rendering and animation. *The Journal of Visualization and Computer Animation 2*, 4 (1991), 141–148.

[RJ07] RIVERS A. R., JAMES D. L.: FastLSM: fast lattice shape matching for robust real-time deformation. *ACM Transactions on Graphics 26* (2007), 82:1–82:6.

[RKN10] RUNGJIRATANANON W., KANAMORI Y., NISHITA T.: Chain shape matching for simulating complex hairstyles. *Computer Graphics Forum 29*, 8 (2010), 2438–2446.

[Rob97] ROBBINS C. R.: *Hair and Hair Care*. Cosmetic Science and Technology Series, 1997.

[Rob02] ROBBINS C. R.: *Chemical and physical behavior of human hair*, fourth ed. Springer, 2002.

[RSKN08] RUNGJIRATANANON W., SZEGO Z., KANAMORI Y., NISHITA T.: Real-time animation of sand-water interaction. In *Computer Graphics Forum (Proc. of Pacific Graphics 2008)* (2008), vol. 27, pp. 1887–1893.

[SBCN10] SILVA P., BANDO Y., CHEN B.-Y., NISHITA T.: Curling and clumping fur represented by texture layers. *Vis. Comput. 26* (2010), 659–667.

[SLF08] SELLE A., LENTINE M., FEDKIW R.: A mass spring model for hair simulation. *ACM Transactions on Graphics 27* (2008), 64:1–64:11.

[ST07] SPILLMANN J., TESCHNER M.: CORDE: Cosserat rod elements for the dynamic simulation of one-dimensional elastic objects. In *Proceedings of the 2007 ACM SIGGRAPH/Eurographics Symposium on Computer Animation* (2007), pp. 63–72.

[VMT06] VOLINO P., MAGNENAT-THALMANN N.: Real-time animation of complex hairstyles. *IEEE Transactions on Visualization and Computer Graphics 12*, 2 (2006), 131–142.

[WBK*07] WARD K., BERTAILS F., KIM T.-Y., MARSCHNER S. R., CANI M.-P., LIN M.: A survey on hair modeling: Styling, simulation, and rendering. *IEEE Transactions on Visualization and Computer Graphics (TVCG) 13*, 2 (2007), 213–234.

[WGL07] WARD K., GALOPPO N., LIN M.: Interactive virtual hair salon. *Presence: Teleoper. Virtual Environ. 16* (June 2007), 237–251.

[WL04] WARD K., LIN M. C.: Modeling hair influenced by water and styling products. In *In International Conference on Computer Animation and Social Agents (CASA* (2004), pp. 207–214.

[WMT05] WANG H., MUCHA P. J., TURK G.: Water drops on surfaces. *ACM Trans. Graph. 24* (2005), 921–929.

[YT10] YU J., TURK G.: Reconstructing surfaces of particle-based fluids using anisotropic kernels. In *Proceedings of the 2010 ACM SIGGRAPH/Eurographics Symposium on Computer Animation* (2010), SCA '10, Eurographics Association, pp. 217–225.